Chemical Science

PERSPECTIVE

View Article Online
View Journal | View Issue

Cite this: *Chem. Sci.*, 2018, **9**, 33

Recent progress on exploring exceptionally high and anisotropic H^+/OH^- ion conduction in two-dimensional materials

Pengzhan Sun, Renzhi Ma * and Takayoshi Sasaki

Ion conducting membranes/electrolytes have been employed extensively in some important industrial and biological systems, especially in fuel cells, water electrolyzers, gas separation, sensors and biological selective ion transport, acting as one of the core components and sometimes directly determining the device performance. However, the traditional polymeric proton exchange membranes (PEMs)/anion exchange membranes (AEMs) suffer from highly toxic preparation procedures, poor thermal and chemical stabilities, and unsatisfactory ion conductivities. This has triggered researchers worldwide to explore alternative inorganic building blocks with high ion conductivities and stabilities from the new materials library, hoping to solve the above long-lasting problems. The recent burgeoning research on two-dimensional (2D) materials has unveiled exceptionally high ionic conductivities, which raises the feasibility of fabricating high-performance nanosheet-based ion conductors/membranes. In this perspective, the recent advances in measuring and understanding the exceptionally high and anisotropic H^+/OH^- ion conductivities of representative 2D materials, *e.g.* graphene oxide (GO), vermiculite and layered double hydroxide (LDH) nanosheets, are reviewed. In particular, regarding the anisotropic ionic conduction in 2D nanosheets, possible design strategies and technological innovations for fabricating macroscopic nanosheet-based ionic conductors/membranes are proposed for maximizing the high in-plane conduction, which may serve to guide future development of high-performance industrial and biological systems relying on H^+/OH^- conducting membranes.

Received 13th September 2017
Accepted 27th October 2017

DOI: 10.1039/c7sc04019a

rsc.li/chemical-science

World Premier International Center for Materials Nanoarchitectonics (WPI-MANA), National Institute for Materials Science (NIMS), 1-1 Namiki, Tsukuba, Ibaraki 305-0044, Japan. E-mail: MA.Renzhi@nims.go.jp

Introduction

The development of highly efficient energy storage and conversion devices independent of fossil fuels has become

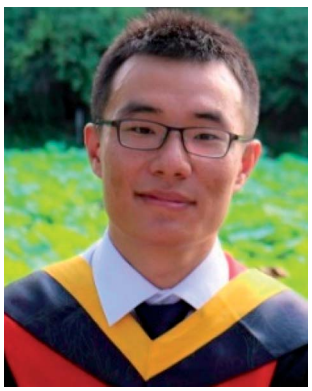

Pengzhan Sun obtained his B.S. degree in Mechanical Engineering and Automation (2012) and Ph.D. degree in Materials Science and Engineering (2016) from Tsinghua University in Beijing, China. During 2015–2016, he was a visiting researcher at the National Institute for Materials Science (NIMS), Japan. He is now a research associate working at the School of Physics and Astronomy, University of Manchester, UK. His research interests include the synthesis and processing of functional 2D nanomaterials (such as graphene, hBN, MoS_2, charge-bearing metallic oxide and hydroxide nanosheets, etc.) and their rationally designed structures for mass transport applications, energy storage and conversion, etc.

Renzhi Ma is an Associate Principal Investigator at the International Center for Materials Nanoarchitectonics (MANA), National Institute for Materials Science (NIMS), Japan. He received his PhD in Materials Processing Engineering from Beijing Tsinghua University in 2000. He worked as a postdoc for three years before becoming a staff researcher at NIMS in 2004. His work focuses on the synthetic chemistry of inorganic 1D nanotubes and 2D nanosheets, and advanced energy storage/conversion materials.

increasingly important toward realizing a clean energy society.[1–3] In this regard, renewable systems such as fuel cells (FCs) have been actively pursued because of their advantages such as high energy conversion efficiency and power density, and low operation temperature and pollutant emission.[4,5] Depending on the type of ion that functions in the FCs, they can be classified into proton exchange membrane fuel cells (PEMFCs) and alkaline fuel cells (AFCs), in which protons and hydroxyl ions are the dominant working ions, respectively. Due to a strong acid environment, the dominant use of high-cost anticorrosive electrodes and precious metallic catalysts presents a primary barrier for PEMFCs to industrial commercialization.[6] By contrast, AFCs employ an alkaline environment, which may significantly reduce the cost due to the feasibility of using non-precious metallic catalysts instead.[7,8] Therefore, the development of high performance AFCs has emerged as a very promising research field in recent years.

In both PEMFCs and AFCs, the H^+/OH^- ion-conducting electrolytes are crucial as conductivities largely determine the performance of FCs. H^+/OH^- ion conductors are also employed extensively in other industrial and biological systems such as water electrolyzers, gas separation, sensors and biological selective ion transport, *etc.* However, on one hand, the traditional polymeric proton exchange membranes (PEMs) and anion exchange membranes (AEMs) usually suffer from highly toxic preparation procedures with poor thermal and chemical stabilities,[9–12] which seriously degrade their safety and durability. On the other hand, due to the lower mobility of OH^- than H^+, the conductivities of AEMs (typically 10^{-3}–10^{-2} S cm^{-1}) are generally lower than those of PEMs (*e.g.* Nafion, 10^{-1} S cm^{-1}),[7,13,14] thus slowing down the technological development as well as the commercialization of AFCs. With this background, the engineering of high-performance inorganic H^+/OH^- ion conductors/electrolytes triggers worldwide research interest.

Recently, inorganic 2D materials[15–19] have provided a forefront for scientists to explore superionic functions. To achieve this purpose, the most straightforward way is to first search and select bulk layered materials possessing H^+/OH^- ion conducting properties. When the dimensionality of layered materials is reduced to their physical limit, the resultant single-layer 2D nanosheets may not only preserve the intrinsic properties of their bulk counterparts, but also be endowed with additional characteristics due to the 2D anisotropy associated with confinement effects.[20–25] Therefore, after isolating single-layer or few-layer nanosheets from their bulk precursors, the ionic conductivities along the nanosheet surfaces or interlayer galleries may be significantly enhanced. On the basis of this research scheme, several types of 2D material such as graphene oxide (GO), vermiculite and layered double hydroxide (LDH) nanosheets have been revealed with promising superionic functions.[26–31] They are emerging as a new class of 2D building block for the construction of high-performance ion conductors/electrolytes for applications such as fuel cells, water electrolyzers, and separation/filtering devices (Fig. 1).

In this perspective, recent advances in exploring the superionic functions of representative 2D materials, *e.g.* GO, vermiculite and LDH nanosheets are reviewed, with a special emphasis on H^+/OH^- ion conductivity measurements and conducting mechanisms (Fig. 1).

When attempting to produce a thin film/membrane, nanosheets almost always spontaneously re-stack in a face-to-face lamellar manner. Novel designs of ion conducting membranes are thus needed to maximize the in-plane conduction of the nanosheets but minimize transport in the perpendicular direction. In this perspective, we will also propose possible design strategies and technological innovations to tackle the anisotropic conducting behavior in fabricating macroscopic ionic conductors/membranes using nanosheets.

Takayoshi Sasaki is the director of the International Center for Materials Nanoarchitectonics (MANA, NIMS). He received his PhD in Chemistry from the University of Tokyo in 1985. Since 1980, he has worked for the National Institute for Research in Inorganic Materials (NIRIM, now NIMS), Japan. In 2009, he was appointed as a NIMS fellow. His recent interest has focused on 2D nanosheets obtained by delaminating layered materials.

H^+/OH^- ion conductivity measurements in 2D materials

Generally, H^+/OH^- ion conductivities in 2D materials are measured either in aqueous solutions or humidified atmospheres.[26–33] In the former case, H^+/OH^- ion conductivities are calculated based on the measured *I–V* curves in strong acids (*e.g.* HCl) and bases (*e.g.* KOH), and finally plotted as a function of H^+/OH^- concentration.[30,32,33] This method is straightforward and the measurement platform is easy to set up. However, H^+/OH^- ion conduction is evaluated in the presence of introduced counter ions (*e.g.* Cl^- in the acidic case and K^+ in the basic case). In the latter case, H^+/OH^- ion conductivities are calculated based on the measured ac impedance spectra in varied humidified atmospheres, and finally plotted as a function of the relative humidity (RH).[26–29,31] The H^+/OH^- ion conduction is driven by the self-dissociation of adsorbed water molecules, which generates protons and hydroxyl ions. Therefore, the system is rather simple, only containing H_2O, H^+ and OH^- without other species, and the ion conduction processes can be precisely controlled by manipulating the water self-dissociation process in a constant temperature and RH chamber.

The 2D structure might bring about highly anisotropic H^+/OH^- ion conduction. In order to clarify this, both the measurements of the in-plane and cross-plane ion conductivities are required. The cross-plane ion conductivity

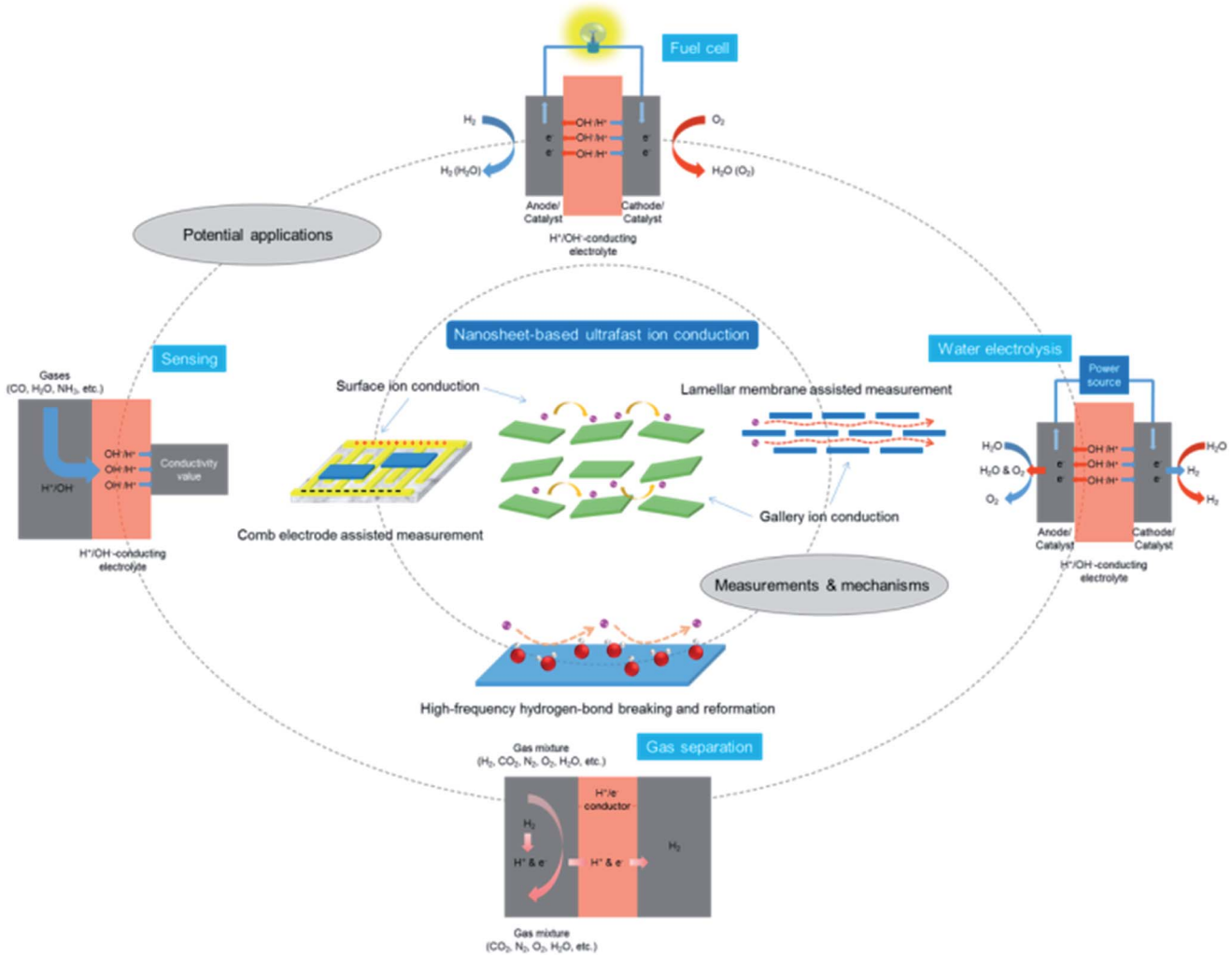

Fig. 1 A schematic diagram for the measurements, mechanisms and potential applications of nanosheet-based ultrafast ion conduction.

measurements can be directly performed in either electrolyte solutions or humidified atmospheres by depositing electrodes on both surfaces of the nanosheet-based freestanding lamellar membrane. In contrast, the in-plane ion conductivity measurements need a more sophisticated technique, which requires the exposure of interlayer galleries or the introduction of electrodes directly on the nanosheet surfaces. In recent papers, two strategies are proposed for the measurement of in-plane ion conductivities: the comb microelectrode-assisted[26–28,31] and lamellar membrane-assisted[30,32,33] methods.

As shown by the schematic diagrams in Fig. 2a (top panels), comb microelectrodes consist of dozens of comb teeth which are connected in parallel, and two identical pairs are arranged alternately. Therefore, when applying a voltage between the two sets of electrodes, the comb teeth connected in parallel are always equivalent in electric potential and only adjacent pairs of comb teeth possess an electric potential difference. The comb electrodes are usually designed with the same width of the comb teeth and the gap between them (a few microns), which is convenient for statistical analysis and calculation. This electrode structure is equivalent to two electrodes deposited with a gap identical to the distance between two adjacent comb teeth and an extremely large length identical to the total length of the comb teeth (Fig. 2a, bottom panels). The only difference is that the comb electrodes are deposited in a folding line manner (as indicated by the blue lines in Fig. 2a) within a limited space, which is beneficial for statistical analysis. Generally, two types of nanosheets, that are deposited discretely on the comb electrodes, can be found: bridging nanosheets and interior nanosheets. Bridging nanosheets connect two or more adjacent teeth whereas interior nanosheets are isolated on an individual tooth or fall right in the gap between two adjacent teeth without an effective connection. According to the electrode structure and its equivalent model, only the bridging ones contribute to the conductivity measurements. Therefore, the bridging nanosheets are counted throughout the sample statistically for calculating the ion conductivity. Due to the limited size of exfoliated nanosheets (generally <10 μm), most bridging nanosheets would connect two adjacent comb teeth. During SEM

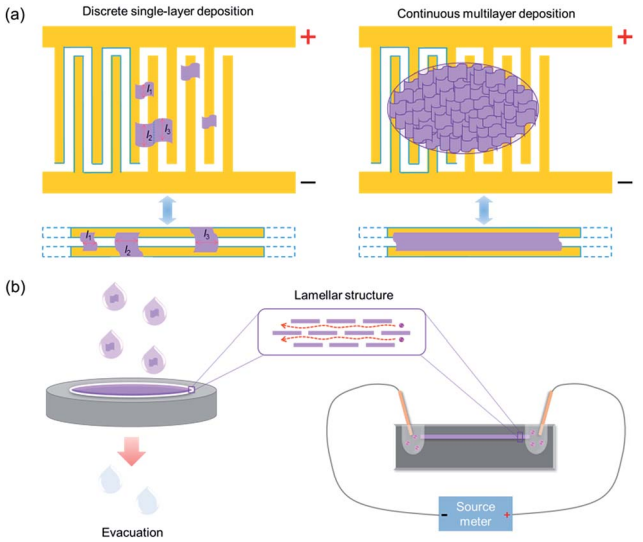

Fig. 2 Schematic diagrams for H^+/OH^- ion conductivity measurements in the case of 2D materials. (a) Comb-like microelectrode assisted measurement and (b) lamellar membrane assisted measurement.

statistics, single-layer nanosheets spanning over three (or more) adjacent comb teeth were rarely observed.[26,27,31]

Similarly, in multilayer depositions, the continuous multilayer film can be treated as an extremely long membrane assembled between two parallel electrodes with a width identical to the distance between two adjacent teeth (Fig. 2a). The length of the membrane can be calculated as $L = S_{film}/2W$, where S_{film} is the area of the multilayer nanosheet film covering the comb electrodes and W is the width between two adjacent teeth. Since the parts located on the comb teeth do not have an effective connection with both electrodes, they can be neglected in ionic conduction. Therefore, only half of the film area should be considered in the length calculation.

On the other hand, the schematic diagrams for the lamellar membrane-assisted measurement are shown in Fig. 2b. The experimental setup usually starts with the preparation of lamellar membranes from nanosheet-containing colloidal suspensions *via* vacuum filtration. After peeling off the free-standing membrane from the filter, it is embedded into a PDMS matrix and sealed. Finally, two reservoirs are punched into the PDMS matrix to expose the fresh edges of the membrane, H^+/OH^- ion-containing electrolytes are introduced and the ion conductivities through the interlayer galleries are measured.

On the basis of the above two measuring techniques, the ion conductivities, through either the surfaces of individual nanosheets or the interlayer galleries of multilayer stackings, were studied, revealing the exceptionally high and anisotropic ion conductivities of several representative inorganic 2D materials such as GO, vermiculite and LDH nanosheets, which will be reviewed in detail in the following sections.

It is noteworthy that in the aforementioned two measurements, the H^+/OH^- ion conductivities were extracted based on either statistical analysis over large quantities of discretely deposited nanosheets or calculation over nanosheet-constructed laminates. Such macroscopic measurements offered reasonable evaluation of the overall ion conductivities. In order to precisely determine the microstructural and 2D H^+/OH^- ion conductivities, direct measurements on individual nanosheets are more desirable. Despite the fact that advanced nanofabrication techniques are required, further efforts should be devoted to this challenging direction since it can provide more genuine and in-depth information on 2D ion conduction processes.

Proton conduction of GO and vermiculite nanosheets

Bearing rich hydrophilic oxygen-containing functional groups (*e.g.* hydroxyl, epoxy and carboxyl) covalently attached on both surfaces of a single-layer graphitic sheet,[34,35] a continuous hydrogen-bonding network can form on the GO nanosheet surface with water molecules in a humidified atmosphere. This endows GO with great possibility to be used as a 2D proton conductor. Given this, Karim *et al.*[26] measured the proton conductivities of single-layer GO nanosheets with the assistance of comb-like microelectrodes. They first discretely deposited single-layer GO nanosheets onto the comb electrodes, as shown in Fig. 3a and b. Then the bridging nanosheets were counted throughout the sample statistically to calculate the proton conductivity of the single-layer sheets according to the measured ac impedances. As shown in Fig. 3c and d, the conductivity exhibited an increasing tendency when both the temperature and relative humidity (RH) were raised. The obtained maximum proton conductivities were in the order of 10^{-2} S cm^{-1} at 95% RH and above 340 K, approaching those of commercial proton conductors such as Nafion. This superionic conductivity was proposed to originate from the attraction of protons by the hydrophilic oxygen functionalities and their subsequent rapid propagation through the hydrogen-bonding network along the adsorbed water layer on the GO surface.

Following this work, Hatakeyama *et al.*[27] deposited multilayer GO nanosheets to form continuous films on comb electrodes, as shown in Fig. 3e. By measuring the conductivities of multilayer films, the thickness-dependent proton conductivities were determined. As shown in Fig. 3f, the measurements of multilayer GO films at different RHs showed that the conductivity increased with film thickness. Below 200 nm thick, the conductivities increased sharply, beyond which a saturation state was observed (Fig. 3g). These results indicate that the multilayer stacking of GO nanosheets to form a compact bundle of 2D proton conduction channels was beneficial for obtaining higher conductivities, presumably originating from the increase of the amount of conduction pathways as well as the improvement in water content and hydration dynamics in multilayer cases that supported an accelerated proton movement and hydrogen bond breaking/reformation process. Notably, by using ethylenediamine (EDA) to selectively block epoxy groups on GO nanosheets and then forming multilayer EDA-modified GO (enGO) films (Fig. 3f), a significant decrease in

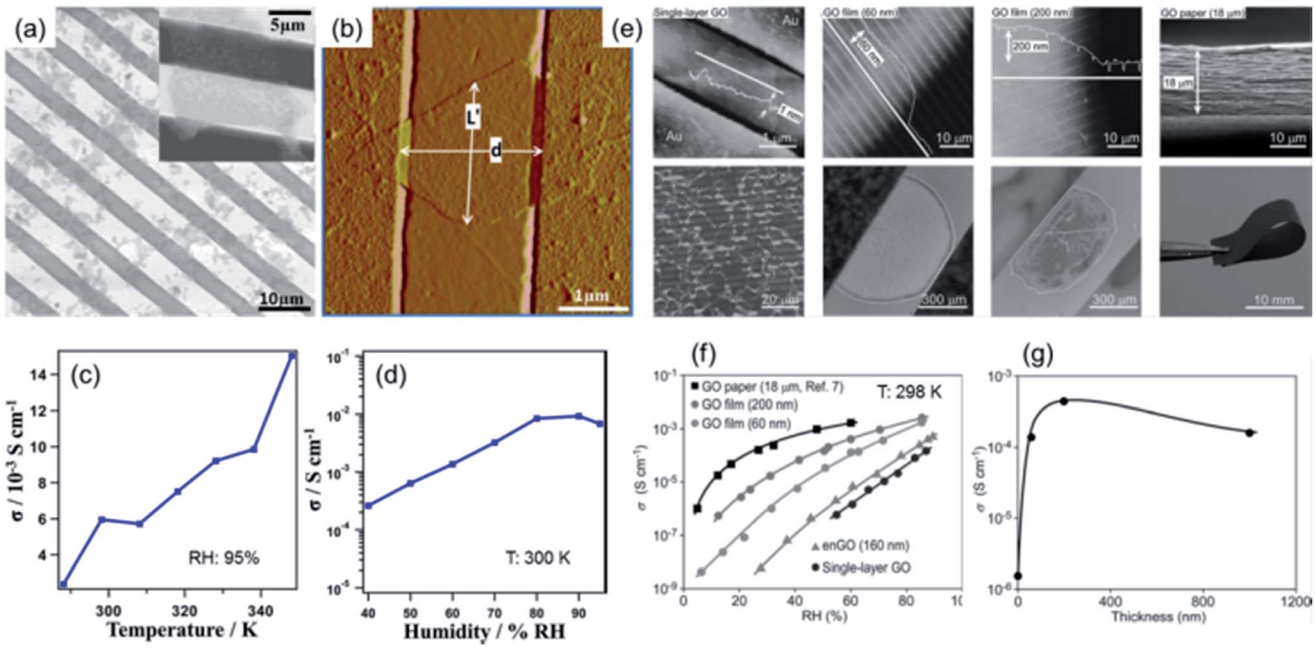

Fig. 3 (a) SEM and (b) AFM images of GO nanosheets deposited on comb-like microelectrodes. (c) Temperature- and (d) RH-dependent conductivities of single-layer GO nanosheets. The RH in (c) was 95% and the temperature in (d) was 300 K. Reproduced with permission.[26] Copyright 2013, American Chemical Society. (e) AFM and SEM images of single-layer and multilayer GO assemblies and their corresponding zoomed-out images. (f) RH-dependent conductivities of single-layer and multilayer GO assemblies at 298 K. (g) Thickness-dependent conductivity variations. Reproduced with permission.[27] Copyright 2014, Wiley-VCH.

conductivity was observed. This result indicates that epoxy groups present on GO might be a major contributor to fast proton conduction. A similar phenomenon has also been observed by Gao *et al.*[29] In their case, the as-prepared GO nanosheets were treated with ozone, which resulted in a higher level of oxidation compared to the pristine state. This treatment also led to a significant increase in proton conductivity, thus demonstrating that a higher content of oxygen functionalities present on GO is beneficial for proton conduction.

The above results indicate that electronically insulating GO nanosheets possess strikingly high proton conductivities. By increasing the operation temperature and RH as well as the GO oxygen content, or by assembling nanosheets into multilayer films, the proton conductivities could be further improved to meet the requirements of high-performance proton conductors for electrochemical energy storage and conversion uses.

Despite bearing superionic functions, GO is a metastable material, and its structure and chemical composition can evolve over time,[36–39] which might lead to the degradation of the high proton-conducting performance during long-term operation. This has motivated scientists to seek other proton-conducting nanomaterials beyond GO with exceptionally high stability in the 2D library. Recently, Shao *et al.*[30] focused their attention on vermiculite, a layered clay mineral, and found that, after exfoliation and reassembly into lamellar membranes, high through-channel (interlayer gallery) proton conductivity and extraordinary thermal stability could be achieved. They first exfoliated vermiculite crystals into few-layer nanosheets *via* thermal shock, interlayer cation exchange and hydrogen peroxide treatment. Through a vacuum-assisted filtration procedure, the as-exfoliated few-layer vermiculite nanosheets were reassembled into flexible and free-standing lamellar films. After sealing the light-brown laminate into a polydimethylsiloxane (PDMS) elastomer and exposing its two ends (Fig. 4a and b), the proton conductivity through the 2D nanofluidic vermiculite channels was measured as a function of the acid concentration in the reservoirs. As shown in Fig. 4c, the proton conductivities of the 2D channels started to deviate from those of the HCl bulk solutions below a concentration of 0.1 M. In this concentration range, the channel conductivity remained stable even if the acid concentration in the reservoirs was varied by orders of magnitude. The stable proton conductivity through the 2D vermiculite channels, generally in the order of 10^{-2} S cm^{-1}, was reasonably high and comparable to that of GO nanosheets. More importantly, as shown in Fig. 4d, even after annealing vermiculite membranes in air for 1 day at 200 and 500 °C, the conductivity did not exhibit any obvious change, showing an exceptionally high thermal stability for the vermiculite channels in terms of proton conduction. These results indicate that vermiculite nanosheets represent another new kind of superionic conducting 2D material with extraordinary thermal stability that is promising for proton-type membrane related applications.

Hydroxyl ion conduction of LDH nanosheets

In recent years, exploring inorganic high hydroxyl ion-conducting materials for fabricating AEMs has emerged as

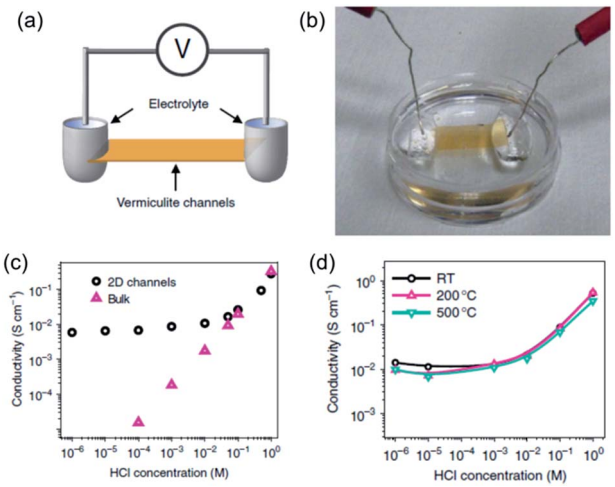

Fig. 4 (a) Schematic drawing and (b) photograph of the experimental setup for measuring the proton conductivity through vermiculite channels. (c) Acid concentration-dependent proton conductivities of vermiculite channels and bulk solutions. (d) Acid concentration-dependent proton conductivities of pristine and 200 °C and 500 °C annealed vermiculite membranes. Reproduced with permission.[30] Copyright 2015, Nature Publishing Group.

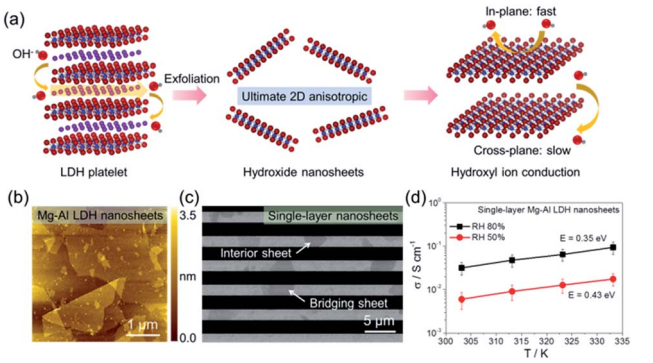

Fig. 5 (a) Schematic drawings of the structure of the LDH platelet, ultimate single-layer nanosheets and hydroxyl ion conduction. (b) AFM characterization of Mg–Al LDH nanosheets. (c) SEM characterization of single-layer Mg–Al LDH nanosheets deposited on comb electrodes. (d) Temperature-dependent in-plane hydroxyl ion conductivities of single-layer Mg–Al LDH nanosheets at 50% and 80% RH. Reproduced with permission.[31] Copyright 2017, The American Association for the Advancement of Science.

a hot yet challenging research topic. LDH[40–42] is a relatively rare class of hydroxyl ion conductor,[43–47] consisting of positively charged hydroxide host layers sandwiched between charge-balancing interlayer anions. However, the hydroxyl ion conductivities of bulk LDHs are typically lower than 10^{-3} S cm^{-1},[43–47] still not high enough for practical use. Through appropriate interlayer anion exchange, followed by mechanical shaking or sonicating in formamide, lamellar LDH platelets can be exfoliated into single-layer nanosheets.[48–52] This raises the feasibility for exploring the possible 2D confinement-correlated hydroxyl ion conduction in the single-layer dimension.

Recently, Sun *et al.*[31] investigated the hydroxyl ion conducting properties of LDH nanosheets. They first synthesized hexagon-shaped lamellar LDH platelets with various bimetallic host layer compositions (*e.g.* Mg^{2+}–Al^{3+}, Co^{2+}–Al^{3+}, Co^{2+}–Co^{3+} and Co^{2+} (Ni^{2+})–Co^{3+}) through well-developed soft-chemical routes.[47–50] After exchanging the interlayer hydrated anions, typically to NO_3^-, LDH precursors were exfoliated into single layers in formamide (Fig. 5a), which were deposited discretely onto comb-like microelectrodes for measuring the in-plane hydroxyl ion conductivities. Fig. 5b shows an atomic force microscopy (AFM) image of as-exfoliated several micrometer-sized single-layer LDH nanosheets. After being deposited onto comb electrodes (Fig. 5c), the bridging nanosheets were counted throughout to calculate the in-plane hydroxyl ion conductivities on the basis of the measured ac impedance spectra. As shown in Fig. 5d, the hydroxyl ion conductivity of single-layer LDH nanosheets increased with temperature and RH. At 80% RH, the in-plane conductivities were generally in the order of 10^{-2} S cm^{-1} and reached 10^{-1} S cm^{-1} at 60 °C. The activation energy for in-plane conduction decreased with the increase of RH, indicating that the presence of water promoted hydroxyl ion conduction. These hydroxyl ion conductivity values were the highest among the state-of-the-art AEMs and comparable to the proton conductivities of commercial PEMs (*e.g.* Nafion), showing promise for single-layer LDH nanosheets as 2D building blocks for constructing high-performance inorganic AEMs.

For comparison, free-standing lamellar membranes composed of overlapped and stacked LDH nanosheets were fabricated and the cross-plane/membrane hydroxyl ion conductivities were measured. In addition, pellet samples containing randomly oriented LDH platelets were fabricated to measure the bulk conductivities. Similarly to the single-layer nanosheets, micrometer-sized hexagon-shaped lamellar LDH platelets were uniformly assembled onto comb electrodes and the conductivities along the plate plane direction were measured. All of the above-mentioned measurements are summarized and schematically shown in Fig. 6a. The obtained conductivities are systematically compared with the in-plane values of the discrete single-layer and continuous multilayer nanosheet assemblies in Fig. 6b. At 60 °C and 80% RH, all of the in-plane conductivities of the nanosheet samples were exceptionally high, in the order of 10^{-2} S cm^{-1} for multilayer cases and 10^{-1} S cm^{-1} for the single-layer case. However, the cross-plane values were ultralow, in the order of 10^{-6} S cm^{-1}. The highly anisotropic hydroxyl ion conduction could be attributed to the structural and morphological anisotropy of 2D nanosheets. On the contrary, the bulk and average conductivities obtained from the pellet samples were in the same order of magnitude as those measured along the plate plane direction on comb electrodes, showing no anisotropic conduction for LDH platelets. The obtained bulk conductivities were generally 1–3 orders of magnitude lower than the in-plane values of the LDH nanosheets, showing the advantage of fully exfoliating layered materials down to the single-layer limit for achieving superionic conducting properties.

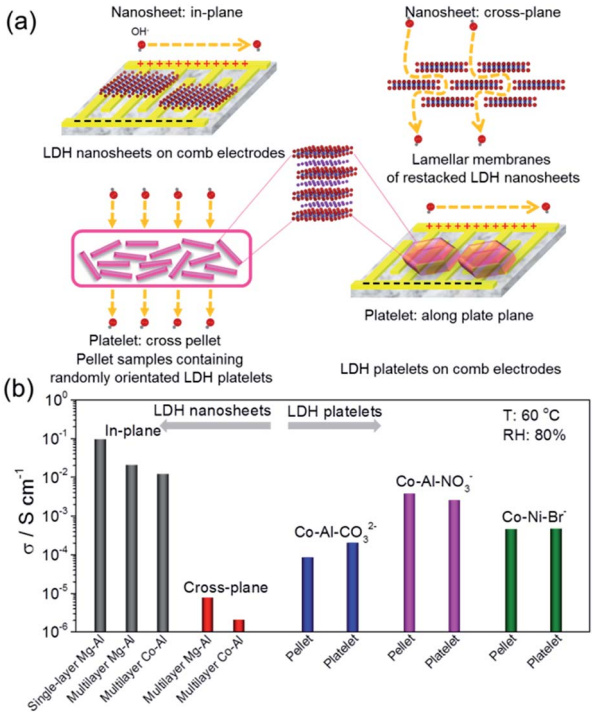

Fig. 6 (a) Schematic drawings for the measurement of different directional hydroxyl ion conductivities for LDH nanosheets and their corresponding bulk precursors. (b) Summary and comparison of the measured conductivities. T: 60 °C and RH: 80%. Reproduced with permission.[31] Copyright 2017, The American Association for the Advancement of Science.

Mechanisms for ultrafast and anisotropic H^+/OH^- ion conduction in 2D materials

For all of the aforementioned 2D materials, the conducting ionic species have been verified. In the vermiculite nanosheet case,[30] the proton conduction was directly confirmed by measuring the ion conductivity using acid (*e.g.* HCl) as the source solution, whereas for GO and LDH nanosheets,[26–28,31] the conducting ion types were distinguished by performing electromotive force measurements as well as isotope effect experiments. At a specific temperature and RH, the conductivity value is inversely proportional to the square root of the conducting isotopic mass. In the GO nanosheet case,[26] the measured conductivity in a H_2O-humidified atmosphere was ~1.25 times higher than that in a D_2O-humidified atmosphere, which agrees well with the above conductivity–isotopic mass relationship, thus confirming that GO nanosheets are proton conductors. By contrast, the difference between the measured conductivities in H_2O and D_2O environments was negligible for LDH nanosheets,[31] indicative of their hydroxyl ion conducting characteristic, presumably because of the tiny mass difference between OH^- and OD^-.

In order to unveil the possible mechanisms for ultrafast and anisotropic ion conduction in 2D materials, the unique 2D structure and chemical composition of nanosheets should be considered first. GO is a non-stoichiometric graphene derivative, the structure of which can be considered as various oxygen functionalities covalently bonded to a carbon atomic sheet. The presence of oxygen functionalities would facilitate rapid proton transport through two routes: (1) charging the GO surface negatively through ionization in a humidified environment, which could attract the positively charged protons efficiently; (2) making the 2D surface rather hydrophilic and facilitating numerous water molecules to firmly attach, which could form a continuous hydrogen bond network along with oxygen functionalities and promote rapid in-plane proton transport through high-frequency hydrogen bond breaking/reformation, *i.e.*, Grotthuss mechanism.

In terms of the structures of bulk vermiculite and LDH, both of them could be treated as charged host layers intercalated with hydrated counterions. The only difference is that the vermiculite host layer is negatively charged while the LDH host layer is positively charged, thus facilitating the attraction of protons and hydroxyl ions, respectively. This might serve as the reason why vermiculite nanosheets are proton conductors and LDH nanosheets are hydroxyl ion conductors. In both nanosheet cases, their surfaces are decorated with densely packed oxygen ions or hydroxyl groups which facilitate the formation of continuous hydrogen bond networks along the 2D surfaces with the assistance of attached water molecules. This hydrogen bond network would promote fast in-plane H^+/OH^- ion conduction through rapid cleavage/reconstruction.

By contrast, for cross-plane H^+/OH^- ion conduction, both the measured conductivities from lamellar GO and LDH nanosheet-based membranes were orders of magnitude lower than the in-plane ones.[29,31,53] This highly anisotropic ion conduction might originate from the structural anisotropy in 2D materials. During cross-plane conduction, ions have to migrate and rely on interlayer hopping, which should result in a much longer conduction pathway and a higher energy barrier when passing through surface pinholes or sheet edges.

In addition, after restacking nanosheets to form lamellar membranes, protons that were produced from the ionization of oxygen functionalities would act as charge-balancing ions in between negatively charged GO nanosheets, and would be rapidly conducting. However, counterions from the interlayer galleries of bulk LDH precursors would accumulate again in as-restacked lamellar LDH membranes in order to balance the positive charges of the host layers. These interlayer anions would cause some electrostatic repulsion to the conducting hydroxyl ions, thus presumably adding extra obstacles for the cross-plane hydroxyl ion conduction in the LDH nanosheet cases. According to previous results,[31,53] the cross-plane proton conductivities in GO nanosheets were generally 1–3 orders of magnitude lower than the in-plane conductivities while the cross-plane hydroxyl ion conductivities in LDH nanosheets were 4–5 orders of magnitude lower than the in-plane values.

The stacking structure-correlated ion conducting characteristics could also be reflected by the in-plane H^+/OH^- ion conductions in multilayer nanosheet assemblies. For GO, the measured in-plane conductivities in multilayer assemblies were orders of magnitude higher than those of single-layer

assemblies.[27] By contrast, the measured in-plane conductivities in multilayer LDH nanosheet assemblies were lower than those of single-layer ones.[31] In GO multilayers, the hydrophilic oxygen functional groups attached on two opposite GO walls would support higher water content as well as a more continuous hydrogen bond network for the interlayer galleries, which could thereby accelerate proton migration and hydrogen bond breaking/reformation. Upon multilayer stacking, more options would be provided for the transporting protons to change pathways, which could also promote fast proton movement. In addition, the interlayer counterions for balancing the negative charges on GO were protons produced from the ionization of oxygen functionalities, which underwent rapid migration themselves in the gallery spacing and would not cause any interference to other propagated protons. Therefore, the in-plane proton conductivities in multilayer GO assemblies were much higher than those in single-layer assemblies. However, in LDH nanosheet multilayers, the charge-balancing guest anions between positively charged LDH nanosheets would sandwich and double in the interlayer galleries, which could compromise the hydroxyl ion conduction due to the increased steric confinement from the narrowed gallery spacing and the enhanced electrostatic repulsion from the crowded interlayer anions. Therefore, the in-plane hydroxyl ion conductivities in multilayer LDH nanosheet assemblies were apparently lower than those in single-layer cases. Nevertheless, when the lateral dimension of the LDH nanosheets was decreased from micrometer size to several hundred nanometer size, the measured in-plane hydroxyl ion conductivities were enhanced,[31] indicating that the more inter-edges produced would create more chances for the propagated hydroxyl ions to change their conduction paths, which could minimize the interference from the interlayer anions and accelerate in-plane transport.

Finally, it is noteworthy that other important factors like temperature, water content/hydration behavior and interlayer spacing could affect the ion conduction along 2D nanosheets. In GO, vermiculite and LDH nanosheets,[26–31] their H^+/OH^- ion conductivities all exhibited an increasing tendency with a raised temperature. Higher temperature promoted H^+/OH^- ion thermal motion as well as water self-dissociation in humidified environments to produce more protons and hydroxyl ions, which was beneficial for achieving higher ion conductivities. As reported in the GO and LDH nanosheet cases,[26–29,31] the ion conductivities increased with RH, indicating that more water molecules originating from higher RH were adsorbed and a higher degree of hydration of the nanosheet surfaces could be achieved, thus providing faster ion conduction channels for the rapid propagation of H^+/OH^- ions. In terms of the interlayer spacing effect, the results for both H^+ conduction in GO[54] and OH^- conduction in LDH[31] showed that a larger interlayer distance could result in higher ion conductivities, presumably because more water molecules would accumulate within a larger gallery spacing to facilitate both ion movement and hydrogen bond cleavage/reformation. In addition, for LDH nanosheets, a larger interlayer distance would provide more space for the propagated OH^- ions to effectively avoid directly facing interlayer guest anions, so as to minimize electrostatic repulsion and increase OH^- ion conductivity.

In short, the 2D structure and chemical composition of nanosheet materials (*e.g.* GO, vermiculite and LDH nanosheets) endow them with exceptionally high and anisotropic ion conducting properties. Generally, the superionic nanosheets are hydrophilic, and could adsorb abundant water molecules onto the surface and form a continuous hydrogen bond network with some specific chemical species (*e.g.* hydroxyl groups) along the host layer. The transported protons or hydroxyl ions are attracted by the surface charges on the nanosheets and undergo rapid propagation *via* the hydrogen bond network through high-frequency hydrogen bond breaking/reformation. This unique ion conduction mechanism indicates that other 2D materials that are capable of forming widely extended hydrogen bond networks with the assistance of adsorbed water or surface chemical species could probably emerge as new superionic 2D materials. This might act as a valuable clue for scientists to explore new kinds of inorganic nanosheets with ultrafast ion conducting properties to enrich the superionic 2D materials library. In addition, some structural and environmental factors like the interlayer distance, temperature and RH were found to significantly affect ion conductivities, which could serve as possible strategies for optimizing ion conduction or even as design criterions for constructing novel structures with superionic functions based on 2D building blocks.

Possible strategies for fabricating macroscopic nanosheet-based ionic conducting membranes

According to the aforementioned H^+/OH^--conducting properties, 2D nanomaterials such as GO, vermiculite and LDH nanosheets exhibit extraordinarily high in-plane ion conductivities. Since the ionic conduction of nanosheets exhibits 2D anisotropy, the conductivity in the direction perpendicular to the sheet surface (film thickness direction) is much lower than that along the sheet surface (in-plane direction).[29,31,53] If such lamellar films are used directly as electrolytes/membranes, the direction perpendicular to the sheet surface (cross-plane) becomes the main pathway for ion conduction, and the in-plane conduction along the sheet surface cannot be effectively utilized. In order to overcome this difficulty, regarding the fabrication of high-performance macroscopic PEMs/AEMs, the highly anisotropic conduction associated with the unique 2D structure should be taken into full account, *i.e.* the ultrahigh in-plane conduction should be maximized whereas the ultralow cross-plane conduction should be minimized. Tackling this challenge needs great technological innovation. Here, we propose several fabrication strategies, which might serve as new development directions for utilizing 2D nanosheets to fabricate macroscopic high-performance ion-conducting membranes, as schematically drawn in Fig. 7.

The above-mentioned three kinds of nanosheet are all charge-bearing, *i.e.* GO and vermiculite nanosheets are negatively charged while LDH nanosheets are positively charged. In

these cases, co-facial alignment of nanosheets yields the maximum electrostatic repulsion as well as nanosheet face-to-face arrangement. Therefore, the first fabrication strategy might be to directionally align nanosheets using strong external stimuli such as electric, magnetic and directional flow fields, followed by transforming the nanosheet dispersion into a hydrogel to fix the transiently induced structural order (Fig. 7a), similar to the recent reports[55,56] of anisotropic hydrogels embedded with co-facially aligned negatively charged monolayer titania nanosheets. Finally the as-prepared hydrogels are cut against the co-facial direction to create thin films with in-plane conduction channels. The key challenges of this strategy might lie in the search for proper external stimuli that are able to directionally align the aforementioned H^+/OH^- ion conducting nanosheets and for suitable hydrogel matrixes that are able to fix the as-aligned 2D nanosheet arrays. In this regard, the fabrication of such an anisotropic nanosheet-based hydrogel membrane with superionic functions is highly challenging and needs more effort. Furthermore, it might provide numerous possibilities in terms of novel behaviors of specific nanosheets under external stimuli as well as unexpected interfacial interactions between nanosheets and hydrogel matrixes.

Due to the structural anisotropy of 2D materials, they tend to adopt a face-to-face stacking manner spontaneously when forming macroscopic structures from their precursor dispersions. In this case, the highly ordered and anisotropic structure has already been formed and the only difficulty that remains is how to fully expose the cross-sections to serve as in-plane channel arrays. To achieve this, two possible strategies are proposed here, both of which involve the fabrication of large-area lamellar membranes composed of overlapped and stacked 2D nanosheets through the well-established liquid-based membrane formation techniques (*e.g.* vacuum-filtration,[57,58] drop-casting,[59,60] spin-coating,[61,62] dip-coating,[63] spraying,[64] layer-by-layer electrostatic assembly[65,66] and Langmuir–Blodgett[67,68]), followed by exposing the fresh in-plane conduction channels through properly scrolling or stacking.

One strategy might be to first scroll the as-prepared nanosheet-based lamellar membranes (with thin polymeric layers on the surfaces acting as binders) into Archimedean spiral fibers (Fig. 7b), similarly to the recent report of preparing layered and scrolled graphene-based nanocomposites,[69] followed by cutting along the direction perpendicular to the fiber axis to produce thin membranes exposed with spiral in-plane conduction pathways. The other strategy might be to first cut the large-area lamellar membranes into pieces, followed by stacking them layer-by-layer with a certain polymer (*e.g.* PDMS) in between as a binder to create a composite embedded with nanosheet lamellar membrane arrays, similarly to the recent investigation of tunable ionic sieving through in-plane GO channels.[70] Finally, the composite would be cut along the stacking direction to produce thin membranes exposed with in-plane conduction channel arrays (Fig. 7c).

The three proposed strategies above might serve as new development directions aiming at making full use of the exceptionally high in-plane ion conductivities of 2D nanosheets. Nevertheless, great effort is certainly needed to realize them for the practical fabrication of macroscopic high-performance ion-conducting membranes.

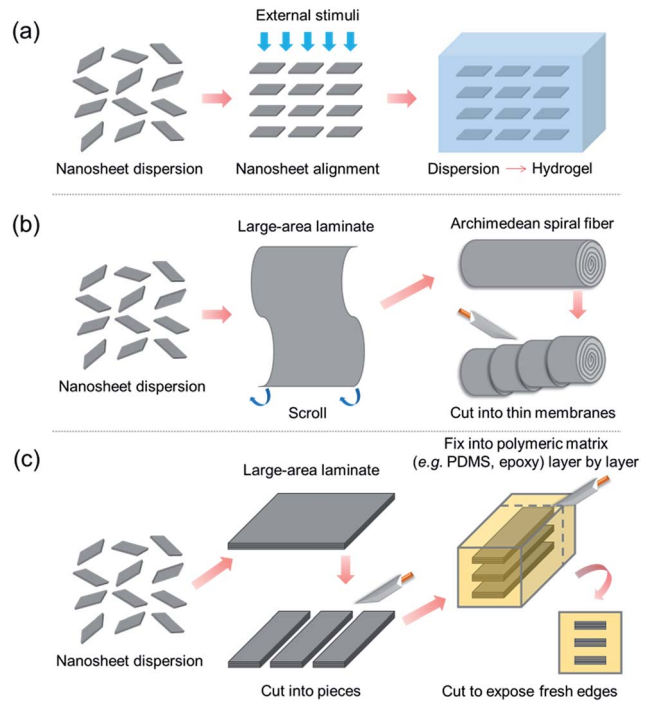

Fig. 7 Schematic diagrams for the proposed strategies to maximize the ultrahigh in-plane ionic conduction of 2D nanosheets. (a) To perpendicularly align and immobilize nanosheets in a matrix by external stimuli. (b) To assemble nanosheets into large-area laminates, scroll into Archimedean spiral fibers and cut into thin pieces perpendicular to the fiber axis. (c) To assemble nanosheets into large-area laminates, cut into pieces and fix them into a polymeric matrix layer by layer, and finally cut again to expose the fresh laminate edges.

Concluding remarks

In summary, dimensionality reduction down to the physical limit brings about exotic properties associated with high anisotropy and confinement effects in 2D materials that are superior to those of or absent in the corresponding bulk counterparts. This has been most markedly highlighted by the recent discoveries of exceptionally high and anisotropic H^+/OH^- conducting properties in GO, vermiculite and LDH nanosheets. On one hand, the ultrahigh in-plane ion conductivities endow these 2D building blocks with great promise to replace the state-of-the-art ion conductors/membranes for further improving device performances. On the other hand, the simultaneously occurring highly anisotropic conduction brings challenges and difficulties for practical fabrication procedures. To tackle this, several strategies for future work have been proposed, which might serve as guidance for fabricating novel ion conducting membranes by taking full advantage of the ultrahigh in-plane ion conducting properties. Despite the fact that research on the discovery and development of superionic 2D nanomaterials is still in the initial stage, sufficient promise has already emerged and future efforts should be devoted to

promoting and maximizing the advantages of these novel superionic 2D building blocks.

Conflicts of interest

There are no conflicts to declare.

Acknowledgements

This work was partly supported by the World Premier International Center for Materials Nanoarchitectonics (WPI-MANA). R. M. acknowledges support from JSPS KAKENNHI (15H03534, 15K13296).

Notes and references

1 Q. Zhang, E. Uchaker, S. L. Candelaria and G. Cao, *Chem. Soc. Rev.*, 2013, **42**, 3127.
2 A. S. Aricò, P. Bruce, B. Scrosati, J.-M. Tarascon and W. van Schalkwijk, *Nat. Mater.*, 2005, **4**, 366.
3 L. Dai, D. W. Chang, J.-B. Baek and W. Lu, *Small*, 2012, **8**, 1130.
4 R. Borup, J. Meyers, B. Pivovar, Y. S. Kim, R. Mukundan, N. Garland, D. Myers, M. Wilson, F. Garzon and D. Wood, *Chem. Rev.*, 2007, **107**, 3904.
5 K. Rajashekara and A. K. Rathore, *Elec. Power Compon. Syst.*, 2015, **43**, 1376.
6 Y. Bing, H. Liu, L. Zhang, D. Ghosh and J. Zhang, *Chem. Soc. Rev.*, 2010, **39**, 2184.
7 G. Merle, M. Wessling and K. Nijmeijer, *J. Membr. Sci.*, 2011, **377**, 1.
8 C. Bianchini and P. K. Shen, *Chem. Rev.*, 2009, **109**, 4183.
9 H. Strathmann, A. Grabowski and G. Eigenberger, *Ind. Eng. Chem. Res.*, 2013, **52**, 10364.
10 H. K. Xu, J. Fang, M. L. Guo, X. H. Lu, X. L. Wei and S. Tu, *J. Membr. Sci.*, 2010, **354**, 206.
11 L. A. Wu, G. F. Zhou, X. Liu, Z. H. Zhang, C. R. Li and T. W. Xu, *J. Membr. Sci.*, 2011, **371**, 155.
12 J. H. Wang, Z. Zhao, F. X. Gong, S. H. Li and S. B. Zhang, *Macromolecules*, 2009, **42**, 8711.
13 Y. J. Wang, J. L. Qiao, R. Baker and J. J. Zhang, *Chem. Soc. Rev.*, 2013, **42**, 5768.
14 G. Couture, A. Alaaeddine, F. Boschet and B. Ameduri, *Prog. Polym. Sci.*, 2011, **36**, 1521.
15 A. K. Geim and I. V. Grigorieva, *Nature*, 2013, **499**, 419.
16 G. R. Bhimanapati, Z. Lin, V. Meunier, Y. Jung, J. Cha, S. Das, D. Xiao, Y. Son, M. S. Strano, V. R. Cooper, L. Liang, S. G. Louie, E. Ringe, W. Zhou, S. S. Kim, R. R. Naik, B. G. Sumpter, H. Terrones, F. Xia, Y. Wang, J. Zhu, D. Akinwande, N. Alem, J. A. Schuller, R. E. Schaak, M. Terrones and J. A. Robinson, *ACS Nano*, 2015, **9**, 11509.
17 H. Wang, H. Yuan, S. S. Hong, Y. Li and Y. Cui, *Chem. Soc. Rev.*, 2015, **44**, 2664.
18 F. Xia, H. Wang, D. Xiao, M. Dubey and A. Ramasubramaniam, *Nat. Photonics*, 2014, **8**, 899.
19 M. Chhowalla, H. S. Shin, G. Eda, L.-J. Li, K. P. Loh and H. Zhang, *Nat. Chem.*, 2013, **5**, 263.
20 K. S. Novoselov, A. K. Geim, S. V. Morozov, D. Jiang, Y. Zhang, S. V. Dubonos, I. V. Grigorieva and A. A. Firsov, *Science*, 2004, **306**, 666.
21 A. H. Castro Neto, F. Guinea, N. M. R. Peres, K. S. Novoselov and A. K. Geim, *Rev. Mod. Phys.*, 2009, **81**, 109.
22 V. Tran, R. Soklaski, Y. Liang and L. Yang, *Phys. Rev. B: Condens. Matter Mater. Phys.*, 2014, **89**, 235319.
23 L. Li, Y. Yu, G. J. Ye, Q. Ge, X. Ou, H. Wu, D. Feng, X. H. Chen and Y. Zhang, *Nat. Nanotechnol.*, 2014, **9**, 372.
24 K. F. Mak, C. Lee, J. Hone, J. Shan and T. F. Heinz, *Phys. Rev. Lett.*, 2010, **105**, 136805.
25 A. Splendiani, L. Sun, Y. Zhang, T. Li, J. Kim, C.-Y. Chim, G. Galli and F. Wang, *Nano Lett.*, 2010, **10**, 1271.
26 M. R. Karim, K. Hatakeyama, T. Matsui, H. Takehira, T. Taniguchi, M. Koinuma, Y. Matsumoto, T. Akutagawa, T. Nakamura, S. Noro, T. Yamada, H. Kitagawa and S. Hayami, *J. Am. Chem. Soc.*, 2013, **135**, 8097.
27 K. Hatakeyama, M. R. Karim, C. Ogata, H. Tateishi, A. Funatsu, T. Taniguchi, M. Koinuma, S. Hayami and Y. Matsumoto, *Angew. Chem., Int. Ed.*, 2014, **53**, 6997.
28 K. Hatakeyama, H. Tateishi, T. Taniguchi, M. Koinuma, T. Kida, S. Hayami, H. Yokoi and Y. Matsumoto, *Chem. Mater.*, 2014, **26**, 5598.
29 W. Gao, G. Wu, M. T. Janicke, D. A. Cullen, R. Mukundan, J. K. Baldwin, E. L. Brosha, C. Galande, P. M. Ajayan, K. L. More, A. M. Dattelbaum and P. Zelenay, *Angew. Chem., Int. Ed.*, 2014, **53**, 3588.
30 J.-J. Shao, K. Raidongia, A. R. Koltonow and J. Huang, *Nat. Commun.*, 2015, **6**, 7602.
31 P. Sun, R. Ma, X. Bai, K. Wang, H. Zhu and T. Sasaki, *Sci. Adv.*, 2017, **3**, e1602629.
32 K. Raidongia and J. Huang, *J. Am. Chem. Soc.*, 2012, **134**, 16528.
33 S. Qin, D. Liu, G. Wang, D. Portehault, C. J. Garvey, Y. Gogotsi, W. Lei and Y. Chen, *J. Am. Chem. Soc.*, 2017, **139**, 6314.
34 G. Eda and M. Chhowalla, *Adv. Mater.*, 2010, **22**, 2392.
35 K. P. Loh, Q. Bao, G. Eda and M. Chhowalla, *Nat. Chem.*, 2010, **2**, 1015.
36 S. Kim, S. Zhou, Y. Hu, M. Acik, Y. J. Chabal, C. Berger, W. de Heer, A. Bongiorno and E. Riedo, *Nat. Mater.*, 2012, **11**, 544.
37 S. Zhou and A. Bongiorno, *Sci. Rep.*, 2013, **3**, 2484.
38 P. V. Kumar, N. M. Bardhan, S. Tongay, J. Wu, A. M. Belcher and J. C. Grossman, *Nat. Chem.*, 2014, **6**, 151.
39 P. Sun, Y. Wang, H. Liu, K. Wang, D. Wu, Z. Xu and H. Zhu, *PLoS One*, 2014, **9**, e111908.
40 R. Allmann, *Acta Crystallogr., Sect. B: Struct. Crystallogr. Cryst. Chem.*, 1968, **24**, 972.
41 P. S. Braterman, Z. P. Xu and F. Yarberry, Layered double hydroxides (LDHs), in *Handbook of layered materials*, ed. S. M. Auerbach, K. A. Carrado and P. K. Dutta, Marcel Dekker Inc., 2004, pp. 373–474.
42 V. Rives, *Layered double hydroxides: Present and future*, Nova Science Publishers Inc., 2006.
43 K. Tadanaga, Y. Furukawa, A. Hayashi and M. Tatsumisago, *Adv. Mater.*, 2010, **22**, 4401.

44 D. Kubo, K. Tadanaga, A. Hayashi and M. Tatsumisago, *J. Power Sources*, 2013, **222**, 493.
45 K. Miyazaki, Y. Asada, T. Fukutsuka, T. Abe and L. A. Bendersky, *J. Mater. Chem. A*, 2013, **1**, 14569.
46 T. Tamaki, N. Nakanishi, H. Ohashi and T. Yamaguchi, *Electrochem. Commun.*, 2012, **25**, 50.
47 L. Zeng and T. S. Zhao, *Nano Energy*, 2015, **11**, 110.
48 T. Hibino and W. Jones, *J. Mater. Chem.*, 2001, **11**, 1321.
49 L. Li, R. Ma, Y. Ebina, N. Iyi and T. Sasaki, *Chem. Mater.*, 2005, **17**, 4386.
50 Z. Liu, R. Ma, M. Osada, N. Iyi, Y. Ebina, K. Takada and T. Sasaki, *J. Am. Chem. Soc.*, 2006, **128**, 4872.
51 R. Ma and T. Sasaki, *Acc. Chem. Res.*, 2015, **48**, 136–143.
52 R. Ma and T. Sasaki, *Adv. Mater.*, 2010, **22**, 5082–5104.
53 H. Tateishi, K. Hatakeyama, C. Ogata, K. Gezuhara, J. Kuroda, A. Funatsu, M. Koinuma, T. Taniguchi, S. Hayami and Y. Matsumoto, *J. Electrochem. Soc.*, 2013, **160**, F1175.
54 M. R. Karim, M. S. Islam, K. Hatakeyama, M. Nakamura, R. Ohtani, M. Koinuma and S. Hayami, *J. Phys. Chem. C*, 2016, **120**, 21976.
55 M. Liu, Y. Ishida, Y. Ebina, T. Sasaki, T. Hikima, M. Takata and T. Aida, *Nature*, 2015, **517**, 68.
56 Y. S. Kim, M. Liu, Y. Ishida, Y. Ebina, M. Osada, T. Sasaki, T. Hikima, M. Takata and T. Aida, *Nat. Mater.*, 2015, **14**, 1002.
57 P. Sun, R. Ma, W. Ma, J. Wu, K. Wang, T. Sasaki and H. Zhu, *NPG Asia Mater.*, 2016, **8**, e259.
58 P. Sun, R. Ma, H. Deng, Z. Song, Z. Zhen, K. Wang, T. Sasaki, Z. Xu and H. Zhu, *Chem. Sci.*, 2016, **7**, 6988.
59 P. Sun, M. Zhu, K. Wang, M. Zhong, J. Wei, D. Wu, Z. Xu and H. Zhu, *ACS Nano*, 2013, **7**, 428.
60 P. Sun, F. Zheng, M. Zhu, Z. Song, K. Wang, M. Zhong, D. Wu, R. Little, Z. Xu and H. Zhu, *ACS Nano*, 2014, **8**, 850.
61 N. N. Nair, H. A. Wu, P. N. Jayaram, I. V. Grigorieva and A. K. Geim, *Science*, 2012, **335**, 442.
62 K. Matsuba, C. Wang, K. Saruwatari, Y. Uesusuki, K. Akatsuka, M. Osada, Y. Ebina, R. Ma and T. Sasaki, *Sci. Adv.*, 2017, **3**, e1700414.
63 X. Wang, L. Zhi and K. Mullen, *Nano Lett.*, 2008, **8**, 323.
64 S. Gijie, S. Han, M. Wang, K. L. Wang and R. B. Kaner, *Nano Lett.*, 2007, **7**, 3394.
65 T. Sasaki, Y. Ebina, T. Tanaka, M. Harada, M. Watanabe and G. Decher, *Chem. Mater.*, 2001, **13**, 4661.
66 L. Z. Wang, Y. Omomo, N. Sakai, K. Fukuda, I. Nakai, Y. Ebina, K. Takada, M. Watanabe and T. Sasaki, *Chem. Mater.*, 2003, **15**, 2873.
67 L. J. Cote, F. Kim and J. Huang, *J. Am. Chem. Soc.*, 2008, **131**, 1043.
68 X. Li, G. Zhang, X. Bai, X. Sun, X. Wang, E. Wang and H. Dai, *Nat. Nanotechnol.*, 2008, **3**, 538.
69 P. Liu, Z. Jin, G. Katsukis, L. W. Drahushuk, S. Shimizu, C.-J. Shih, E. D. Wetzel, J. K. Taggart-Scarff, B. Qing, K. J. Van Vliet, R. Li, B. L. Wardle and M. S. Strano, *Science*, 2016, **353**, 364.
70 J. Abraham, K. S. Vasu, C. D. Williams, K. Gopinadhan, Y. Su, C. T. Cherian, J. Dix, E. Prestat, S. J. Haigh, I. V. Grigorieva, P. Carbone, A. K. Geim and R. R. Nair, *Nat. Nanotechnol.*, 2017, **12**, 546.